

## NASA's Cyclone Global Navigation Satellite System (CYGNSS) Mission – Temporal Resolution of a Constellation Enabled by Micro-Satellite Technology

Randy Rose, Will Wells, Jillian Redfern, Debi Rose, John Dickinson  
Southwest Research Institute  
6220 Culebra Rd, San Antonio TX; 210-522-3315  
rrose@swri.org

Chris Ruf, Aaron Ridley  
University of Michigan  
2455 Hayward St, Ann Arbor MI; 734-764-6561  
cruf@umich.edu

Kyle Nave  
Applied Defense Solutions  
10440 Little Patuxent Parkway, Suite 600 | Columbia, MD; 410-715-0005  
knave@applieddefense.com

### ABSTRACT

Hurricanes Katrina and Irene, each in their own way, are stark examples that while tropical storm track forecasts have improved in accuracy by ~50% since 1990, there has been essentially no improvement in the accuracy of the storm's intensity prediction. In both cases, forecasters predicted almost exactly where the storms would make landfall, but failed to predict the storm's intensity. Principle deficiencies of current tropical cyclone intensity forecasts lie primarily with inadequate observations and modeling of the inner core. The inadequacy in observations results from two causes: 1) Much of the inner core ocean surface is obscured from conventional remote sensing instruments by the storm's intense precipitation. 2) The rapidly evolving (genesis and intensification) stages of the TC life cycle are poorly sampled in time by conventional polar-orbiting, wide-swath surface wind imagers.

NASA's Earth science mission, the Cyclone Global Navigation Satellite System (CYGNSS) is being designed to address tropical storm intensity forecast deficiencies by combining the all-weather performance of GNSS bi-static ocean surface scatterometry with the sampling properties of a satellite constellation. CYGNSS will demonstrate how micro-satellite technology can be applied to provide low cost solutions to fill capability voids in existing large-scale observatories.

An overview will be presented of the CYGNSS mission, its science objectives, and how the use of a micro-satellite constellation results in sampling properties that are markedly improved beyond conventional wind speed observatories.

### OVERVIEW

The NASA EV-2 Cyclone Global Navigation Satellite System (CYGNSS) is a spaceborne mission focused on tropical cyclone (TC) inner core process studies. TC track forecasts have improved in accuracy by ~50% since 1990, largely as a result of improved mesoscale and synoptic modeling and data assimilation, while in that same period there has been essentially no improvement in the accuracy of intensity forecasts. This fact is widely recognized not only by national research institutions [1, 2] but by the popular press as well [3]. The fact that forecast improvements in TC intensity have lagged so far behind those of TC track suggests that the deficiency lies somewhere other than proper

observations and modeling of the mesoscale and synoptic environment. CYGNSS mission objectives and requirements have been defined to address principle deficiencies of intensity forecasts; inadequate observations and modeling of the storm's inner core.

Inadequate observations result from two causes: 1) Much of the inner core ocean surface is obscured from conventional remote sensing instruments by intense precipitation in the eye wall and inner rain bands. 2) The rapidly evolving (genesis and intensification) stages of the TC life cycle are poorly sampled in time by conventional polar-orbiting, wide-swath surface wind imagers. CYGNSS addresses these two

limitations by combining the all-weather performance of GNSS bistatic ocean surface scatterometry with the sampling properties of a constellation of satellites [4, 5]. The use of a dense constellation of micro-observatories results in spatial and temporal sampling properties which are markedly different from conventional imagers. A low-cost micro-satellite and GNSS receiver design are used which could practically be used in an affordable global constellation mission. Compromises in some aspects of the design are necessary (e.g. limiting the downward looking antenna gain) in order to keep the system small and affordable. The paper also outlines constellation deployment and configuration management issues that CYGNSS address.

## MISSION DESIGN

CYGNSS measures the ocean surface wind field with unprecedented temporal resolution and spatial coverage, under all precipitating conditions, and over the full dynamic range of wind speeds experienced in a TC. It does so by combining the all-weather performance of GPS-based bistatic scatterometry with the sampling properties of a dense microsatellite constellation. Near-surface winds over the ocean are major contributors to and indicators of momentum and energy fluxes at the air/sea interface. Our goal, to understand the coupling between the surface winds and the moist atmosphere within a TC, is key to properly modeling and forecasting its genesis and intensification.

Surface wind fields of the TC inner core, including regions beneath the intense eye wall and rain bands that could not previously be measured from space will be provided by CYGNSS. Mission simulation studies predict a mean revisit time of 4.0 hrs. The CYGNSS wind fields, when combined with as-frequent precipitation fields (e.g. produced by the upcoming Global Precipitation Measurement (GPM) core satellite and the current constellation of precipitation imagers), image the evolution of both the precipitation and underlying wind fields throughout the complete TC life cycle. They provide coupled observations of moist atmospheric thermodynamics and ocean surface response, and enable new insights into TC inner core dynamics and energetics.

The use of a space-based constellation results in spatial and temporal sampling properties that are markedly improved from conventional wide swath polar imagers. All previous space-based measurements of ocean surface vector winds have suffered from degradation in highly precipitating regimes. As a result, in the absence of reconnaissance aircraft, the accuracy of wind speed estimates in the inner core of the hurricane is often highly compromised. The added quality and quantity of

surface wind data provided by CYGNSS in precipitating conditions significantly improves estimates of intensity. The orbits of present space-based active and passive microwave observatories maximize global coverage but can result in large gaps in the tropics [6]. The irregular and infrequent revisit times (ca. 11-35 hrs) are likewise not sufficient to resolve synoptic scale temporal variability. Missed core imaging events can occur when an organized system passes through an imager's coverage gap or when its motion is appropriately offset from the motion of the imager's swath.

Each CYGNSS Observatory consists of a microsatellite (commonly referred to as a "usat") platform hosting a GNSS receiver modified to measure surface reflected signals. Similar GNSS-based instruments have been demonstrated on both airborne and spaceborne platforms to retrieve wind speeds as high as 60 m/s (a Category 4 hurricane) through all levels of precipitation, including the intense levels experienced in a TC eyewall [4]. Each Observatory simultaneously tracks scattered signals from up to four independent transmitters in the operational GPS network. The number of CYGNSS Observatories and orbit inclination are chosen to optimize the TC sampling properties. The result is a dense cross-hatch of sample points on the ground that cover the critical latitude band between  $\pm 35^\circ$  with an mean revisit time of 4.0 hrs.

### *Baseline Design Performance*

The performance of the baseline mission design was developed using a time-dependent overlay of the simulated CYGNSS sampling characteristics onto a database of storm tracks for every TC that occurred during the 2003-2007 Atlantic hurricane seasons. A total of 84 TCs were recorded during this period, making it an excellent population with which to determine the statistical properties of our performance. The overlay accounts for the relative orbital motion of each CYGNSS observatory as well as the trajectory of every TC. It predicts where and when every sample of every TC would have occurred if CYGNSS had been in orbit during 2003-2007. From this data, detailed coverage statistics are derived. Parametric sensitivity analysis of the dependence of CYGNSS performance on various mission design variables was conducted using a time-independent overlay. In this case, all CYGNSS spatial samples made in a 24 hr period were overlaid onto a compiled record of all named storm tracks (with wind speeds >30 kts) from 2000-2009.

*Number of Observatories*—The 24 hr storm coverage statistic is shown in Figure 1 as a function of the number of Observatories lost from the initial constellation. The result from the time-dependent

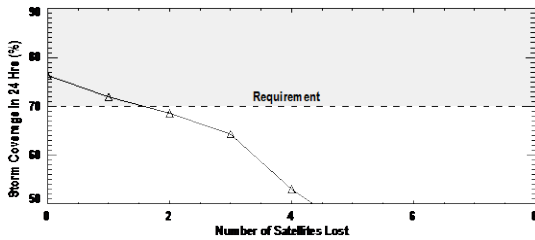


**Figure 1 - Dependence of 24 hr coverage on number of Observatories lost. The 70% storm coverage requirement is met by 7 or more Observatories.**

analysis – that 7 are sufficient but 6 are not – is consistent with a time-independent requirement of 70% or more 24 hr storm coverage. For this reason, the value of 70% is used as a time-independent proxy for the time-dependent requirement.

**Orbit Altitude**—Altitude can affect coverage in competing ways. As altitude increases, the projected antenna footprint on the ground grows, increasing the potential number of observable GPS reflections. Increasing altitude also lengthens the propagation path and lowers received signal strength, thus narrowing the usable solid angle of the antenna pattern. The increase in footprint size would dominate if the number of observable reflections was allowed to grow. However, because the Delay Doppler Mapping Instrument (DDMI) can simultaneously observe a maximum of only 4 reflections, coverage does not improve much above an altitude of ~350 km. Coverage begins to decrease due to the longer propagation path above ~550 km. The baseline altitude of 500 km satisfies the mission lifetime requirement while staying within the broad range indicated by this coverage analysis.

**Orbit inclination**—Inclination affects storm coverage in two ways. Very low inclination angles reduce coverage because the prevailing latitudinal “corridors” favored by tropical storms become under-sampled or missed altogether. Inclination angles too far above these preferred latitudes also tend to decrease coverage because more time is spent over mid-latitude regions with a low probability of TC occurrence. These competing dependencies are shown in Figure 2. The baseline mission design of 35° is located at the center of a broad maximum in coverage.

**MISSION IMPLEMENTATION**

CYGNSS is enabled by technology with nanosat heritage and serves as a prime example of applying a low-cost constellation to fill a gap data provided by existing monolithic observatories [7]. Mission implementation involves a simple nadir-pointed Observatory hosting an instrument technically proven on orbit. Required global coverage is provided by 8

Observatories dispersed about a 500 km, 35° circular orbit. After commissioning and engineering operations are completed, the Observatories are placed into nominal Science mode, where they operate continuously with no instrument commanding required except for bi-annual engineering calibration operations. The simple mode flow is illustrated in Figure 3.

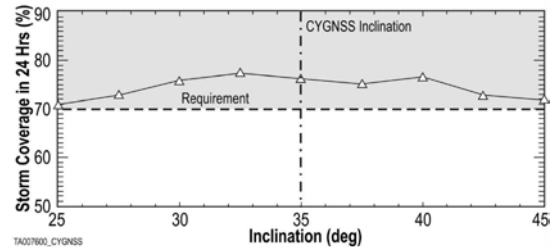


**Figure 2 - Dependence of 24 hr coverage on orbit inclination angle. 35° baseline inclination is centered in a broad maximum of storm coverage dependence, leaving a wide margin for inclination angle variations, if needed**

While the constellation is central to meeting science requirements, the individual Observatories act independent of one another, with no need to synchronize with the other Observatories. They are identical in design but provide their own individual contribution to the CYGNSS science data set. The Observatory consists of the DDMI integrated with the µsat. The Deployment Module (DM), in combination with the launch vehicle (LV), deploys the Observatories into their proper initial orbit configuration. The CYGNSS system is designed to reduce operational overhead of the CYGNSS Observatories during normal science operations to alleviate configuration control issues associated with standard spacecraft and provide a more efficient operational scenario for the constellation.

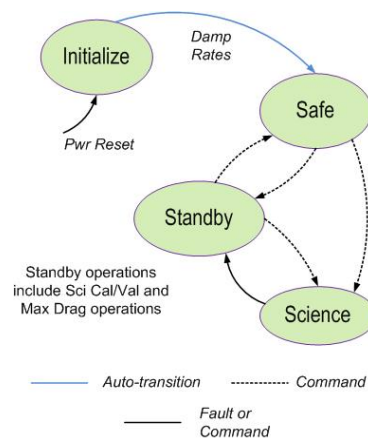


**Figure 3 - Observatory mode flow**

### Technology Basis

Fig. 2 (left) illustrates the propagation and scattering geometries associated with GNSS ocean surface scatterometry. The direct GPS signal provides a coherent reference for the coded GPS transmit signal received by an antenna on the zenith side of the spacecraft. The quasi-specular forward scattered signal from the ocean surface is received by a downward looking antenna on the nadir side of the  $\mu$ sat. The scattered signal contains detailed information about the reflected ocean surface roughness statistics, from which local wind speed can be derived [8]. The scattering cross-section image produced by the UK-DMC-1 demonstration spaceborne mission is shown in Fig. 21 (right). Variable lag correlation and Doppler shift, the two coordinates of the image, enable the spatial distribution of the scattering cross-section to be resolved [9, 10]. This type of scattering image is referred to as a Delay Doppler Map (DDM). The arc represents the departure of the actual bi-static scattering from the purely specular case that would correspond to a perfectly flat ocean surface, which appears in the DDM as a single point scatter.

### Operational Concept

*Launch and Early Operations*—The launch configuration is comprised of the 8 Observatories mounted on a DM in 2 tiers of 4 Observatories (Figure 4). A single LV is used to minimize launch costs of the CYGNSS mission. Use of a single LV causes risk of collision during minimum conjunction 1/2 orbit after separation. A Monte Carlo analysis was performed to design a DM-Observatory separation sequence to ensure a minimum 1/2 orbit conjunction of  $>1$ km. The sequence configuration included cross-track orientation, delay between separating Observatory pairs, and Observatory separation velocity. The LV and DM deploy the Observatories in opposite pairs to balance forces imparted on the LV control system.

The results of the analysis yielded a DM-Observatory separation sequence configuration that provides a minimum conjunction of  $>1.5$ km and a mean of 2.7km.

After DM separation, the Observatories autonomously recover from any deployment tipoff rates and orient themselves into a safe sun-pointing configuration within 3 orbits. This configuration provides significant power margins and allows the Observatory to remain indefinitely with their S/A stowed. S/A deployment is initiated via ground command during communication passes nominally within the first 14 orbits after deployment. The Observatories then enter the commissioning phase of operations where they are

placed into an orbit in an interleaved fashion and the operational orbit configuration is established.

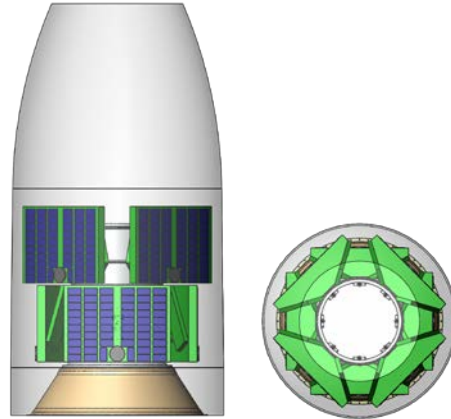


**Figure 4 - Launch configuration of the CYGNSS constellation**

### Constellation Orbital Configuration

After deployment, there are a number of different options for how the constellation of eight observatories can orbit Earth relative to each other. One option is not to control the configuration and allow the different velocities imparted by deployment to determine their orbit state. This would result in all satellites having slightly different orbit periods and result in a dynamic configuration of satellites that constantly changes over time. The other option is to specify a desired end state and control to this desired end state. A controlled configuration offers a number of spacing options that can be exploited to address specific mission science objectives and requirements.

The benefits of an uncontrolled constellation are that there are no maneuvers required to establish the desired constellation configuration or to maintain it. The downside is that over time the constellation configuration is undetermined and the science coverage will change over time in an unpredictable fashion. When the Observatories cluster together, they start measuring similar areas over the ocean, thereby reducing science coverage and resulting at times in coverage that does not meet mission requirements (reference Figure 5). The controlled constellation requires the calculation of maneuvers to establish and then maintain the configuration, but provides predictability to the constellation for science coverage. The configuration can also be selected to “tune” competing science coverage metrics such as percent area coverage and revisit rate. The CYGNSS team has developed a set of tools, based on high fidelity STK<sup>®</sup> scenarios that have been used to explore a number of

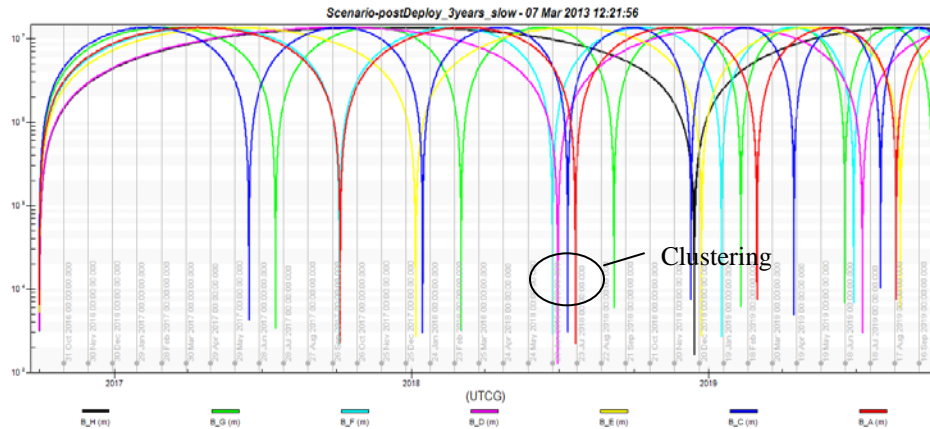


**Figure 5 - Observatory separation distances for mission given no orbital position control. Points of conjunction are identified with significant clustering occurring several times during the mission.**

potential configurations to assess the impact on science coverage.

#### *Orbital Control*

Cost constraints of the CYGNSS mission preclude inclusion of velocity thrusters on the Observatories. Although the satellites do not have thrusters, a Delta-V can be realized by pitching the vehicle to increase its drag area relative to the other vehicles. This technique, known as "differential drag", results in an increased drag profile that results in an acceleration opposite the velocity vector which can be used to adjust the relative position of the satellites and to avoid potential conjunctions [11]. The unique physical configuration of the CYGNSS Observatory provides an excellent 7:1 drag profile that can be exploited to control the constellation orbital configuration with minimal impact to CYGNSS operational life expectations.

#### *Constellation Maintenance*

After the constellation orbital configuration has been established, it will be disturbed in one of two ways; atmospheric drag variations and space object avoidance.

*Atmospheric drag variance*—The uncertainties in vehicle state and the imperfect ability to control the vehicle state mean that there will be a very small relative drift rate between the observatories that will eventually grow to a large error that we would want to correct. This will occur over a period of a number of months to years depending on selected tolerance.

*Conjunction Assessment (CA)*—The other source of disturbance is maneuvers required to avoid conjunctions with other space objects. Studies have shown that conjunction events will happen frequently enough to be the dominant factor in determining when

CYGNSS Observatory orbital maneuvers will occur. There are currently over 13,700 objects in the unclassified space catalog of which about 1900 of them are presumed to be active. Most of these objects reside in Low Earth Orbit (below 2000 km) with a peak density around 800 km caused by a combination of the Fengyun-1C debris and the Iridium-Cosmos collision. Monte Carlo studies have been performed to assess the expected frequency of conjunction events within a given threshold minimum range. The study assumed that the current catalog of space objects is representative of the environment that CYGNSS will encounter during operations. The results of the study show that there will be regular (i.e. weekly) encounters within 2 km and somewhat more infrequent encounters (monthly or less) within 0.5 km.

Due to the large uncertainty in object state, there will likely be a daily process to assess incoming data from the Joint Space Operations Center (JSpOC) for potential conjunctions even though actual conjunctions that require maneuvers will be rare.

Each conjunction event will be evaluated to determine a probability of conjunction. A threshold will be established to determine when a maneuver will be required to decrease the probability below the defined threshold. There will be competing requirements at this point as the uncertainty in vehicle state at the time of close approach (TCA) will be decreasing as the TCA approaches however due to limited ability to affect vehicle state through drag maneuvers, maneuvers will need to occur as soon as possible to have the greatest ability to decrease the probability of conjunction. Ongoing studies will determine the desired window within which to perform a maneuver relative to TCA and the duration of the required window. Initial studies show that maneuvers that occur two days prior to TCA with a duration of one day are sufficient to handle

almost any encounter. A typical maneuver of this duration will result in a drop in semi-major axis (SMA) of about 0.16 km. During operations, specific encounters will be evaluated and maneuver plans will be developed that minimize this loss of altitude while still resulting in a collision probability below the acceptable threshold.

*Science Operations*—Following commissioning, the instrument is set to Science mode for the duration of the mission, except for brief returns to engineering verification performed bi-annually. In Science mode, science measurements are acquired and downlinked with 100% duty cycle. The Observatories are designed to implement nominal Observatory operations and science data collection without on-board schedule command sequences.

## OBSERVATORY IMPLEMENTATION

### *Delay Doppler Mapping Instrument*

CYGNSS accomplishes its science goal using a Delay Doppler Mapping Instrument (DDMI) on each Observatory. The CYGNSS DDMI uses Surrey’s off-the-shelf GNSS Receiver-Remote Sensing Instrument (SGR-ReSI), an upgraded version of the UK-DMC-1 instrument that flew in 2003. The upgrades include a new GPS front end MMIC receiver and the addition of a digital signal processing back end. The new front end improves noise performance, adds internal calibration, and raises the digital sample rate. The new back end adds more on-board processing capacity in order to raise the duty cycle of science operations.

In total, the DDMI consists of the Delay Mapping Receiver (DMR) electronics unit, two nadir-pointing antennas for collecting reflected GNSS signals, and a zenith-facing antenna providing space-geolocation capability.

DDMI onboard processing generates maps of GPS signals scattered from the ocean surface. These are referred to as Delay Doppler Maps (DDMs). The coordinates of a DDM are Doppler shift and time delay offset relative to the specular reflection point of the GPS signal. Each pixel of the DDM is obtained by cross-correlation of the received signal with a locally generated replica time delay and Doppler shift. An open-loop tracking algorithm allows each DDM to be processed by predicting the position of the specular reflection point from the known positions of the receiver and GPS transmitter. Each DDM has 128 delay pixels with resolution of 61 ns. The Doppler resolution is 250 Hz over a  $\pm 6.5$  kHz range, resulting in 52 Doppler pixels.

Available hardware resources allow generation of four simultaneous DDMs. The output data rate is determined by onboard coherent and incoherent integration. The coherent (complex signal) integration time is limited to 1 ms by the rate of change of the propagation geometry due to receiver motion. Individual complex DDMs are then incoherently integrated (magnitude only) for 1 s to form the final DDM. Incoherent integration reduces noise due to speckle and improves the signal-to-noise ratio (SNR). The incoherent integration time is limited to 1 s due to the degradation in spatial resolution caused by along-track smearing.

### *Instrument Accommodation*

While not challenging, instrument accommodation and LV compatibility requirements drive the  $\mu$ sat requirements, resulting in an integrated  $\mu$ sat-DDMI solution that meets all science requirements and allows use of the available NASA NLS-II launch services.

*Configuration*—DDMI antenna pointing constraints drive the overall Observatory physical configuration. The dependence of science coverage requirements on the tilt and rotation pointing angles of the antenna boresight was determined using the CYGNSS mission simulator. Figure 6 illustrates that the dependence of storm coverage on antenna tilt, or roll about the x-axis, is minimal. Figure 7 shows that the coverage dependence on antenna rotation, or yaw about the z-axis, is also minimal. A wide range of antenna configurations were analyzed to meet the science requirements for 70% 24 hr storm coverage with a <12 hr mean revisit tempo. A tilt angle of 28° and rotation

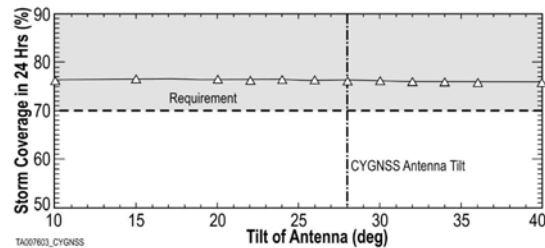


**Figure 6 - Antenna tilt analysis demonstrates design trade space to accommodate manufacturing tolerances and performance improvements if necessary**

angle of 60° were chosen to optimize Observatory close packing and accommodation on the Deployment Module (DM) during launch. The relative insensitivity of spatial coverage to antenna pointing relaxes several other requirements. Mechanical tolerances on the alignment between the electrical boresight of the antenna and the optical boresight of the attitude determination sensor can be relaxed, as can the control of the  $\mu$ sat attitude itself while on orbit.



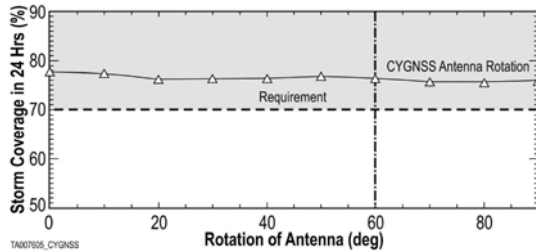


**Figure 7 - Antenna rotation analysis results illustrate key configuration decision effects on science performance**

*Pointing*—Pointing knowledge uncertainty directly translates into an uncertainty in the antenna pattern gain in the direction of the specular reflection point producing an uncertainty in calibration of the scattering cross-section needed to estimate wind speed. Given the science requirement for wind speed error of  $<2$  m/s or 10% of the wind speed (whichever is greater), we have allocated 65% of the error budget as the pointing knowledge requirement to accommodate other physical error sources. A pointing knowledge uncertainty requirement of  $2.7^\circ$  ( $3\sigma$ ) translates into a max absolute error of 0.8 m/s for wind speeds below 20 m/s and a 6.2% max relative error for wind speeds between 20 and 60 m/s (Figure 8).

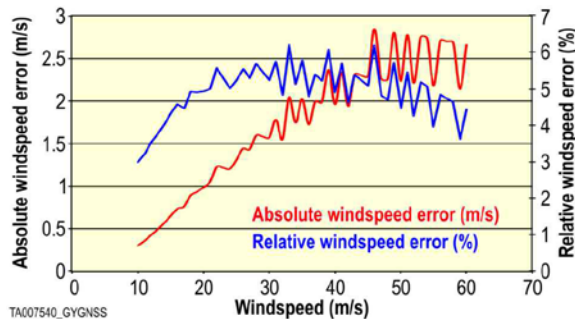


**Figure 8 - Wind speed error due to  $2.7^\circ$  ( $3\sigma$ ) pointing knowledge uncertainty**

Pointing control is not critical with primary considerations derived from providing a nadir reference and minimizing signal path loss due to cosine losses. We conservatively require  $5^\circ$  ( $1\sigma$ ) control of antenna pointing relative to  $\mu$ sat nadir.

Pointing stability and jitter requirements are derived from the DDM processing requirement. The DDM is formed by coherent integration over 1 ms, followed by incoherent averaging of 1000 DDMs to improve SNR. The coherent integration requires that the image be stable to 1/10 the order of the DDM resolution, whereas the incoherent integration requires pointing stability on

the order of the resolution. The spatial extent of the DDM covers  $\sim 100 \times 100$  km and is sampled every 1 km. The nominal range of  $\sim 1000$  km from the Observatory to the specular reflection point corresponds to a subtended angle of 0.001 radian/pixel. The pointing jitter is required over a coherent integration time (1 ms) to be no more than 1/10 of the pixel size ( $20''/\text{ms}$ ), and the stability over the incoherent integration time (1 s) is required to be no more than one half the pixel size ( $100''/\text{s}$ ). As a result, the short term pointing jitter has a negligible effect on the science data processing.

*On-board Data Handling*—The CYGNSS mission is enabled by the DDMI capability to convert raw I/Q data to Delay Doppler Maps (DDM), but even the heritage DDM processing requires further on-board data volume reduction to meet downlink limitations of the microsatellite. The fully resolved DDM from the DDMI contains many highly correlated image pixels, as well as many pixels that do not contain information about the local wind field in the scattering region. In order to reduce the downlink data rate, an onboard image sub-sampling algorithm is used prior to data downlinking providing a 47:1 reduction in the DDM data size, resulting in a total data downlink volume of 95.2 MB/2 days. The DDMI also outputs CYGNSS Observatory ephemerides for  $\mu$ sat position knowledge and GNSS ephemerides for DDM geo-referencing.

*Power*—The DDMI requires 12 W at 28 V for science data collection. Stand-by mode is not necessary as the unit can be turned off while not in use and requires minimal warm-up time when powered ON. Data collection starts after  $\sim 5$  min, when the unit has acquired the necessary GPS satellites.

#### Microsatellite

The CYGNSS  $\mu$ sat is based on a single-string hardware architecture (Figure 9) with functional and selective redundancy included for critical areas. The  $\mu$ sat has been designed from the beginning for ease of manufacture, integration, and test to provide a low-risk, cost-effective solution across the constellation.

*Structure and Thermal*—The nanosat’s shape as illustrated in Figure 10 is specifically configured to allow clear nadir and zenith FOV for the nadir and zenith GNSS antennas, while its structure integrates the nanosat and instrument electronic boards directly by creating avionics and GNSS Receiver “bays”. The avionics and GNSS receiver bays form the core of the nanosat; all other components are mounted to this backbone with structural extensions included to accommodate the Al honeycomb-based S/As and nadir GNSS antenna assemblies.

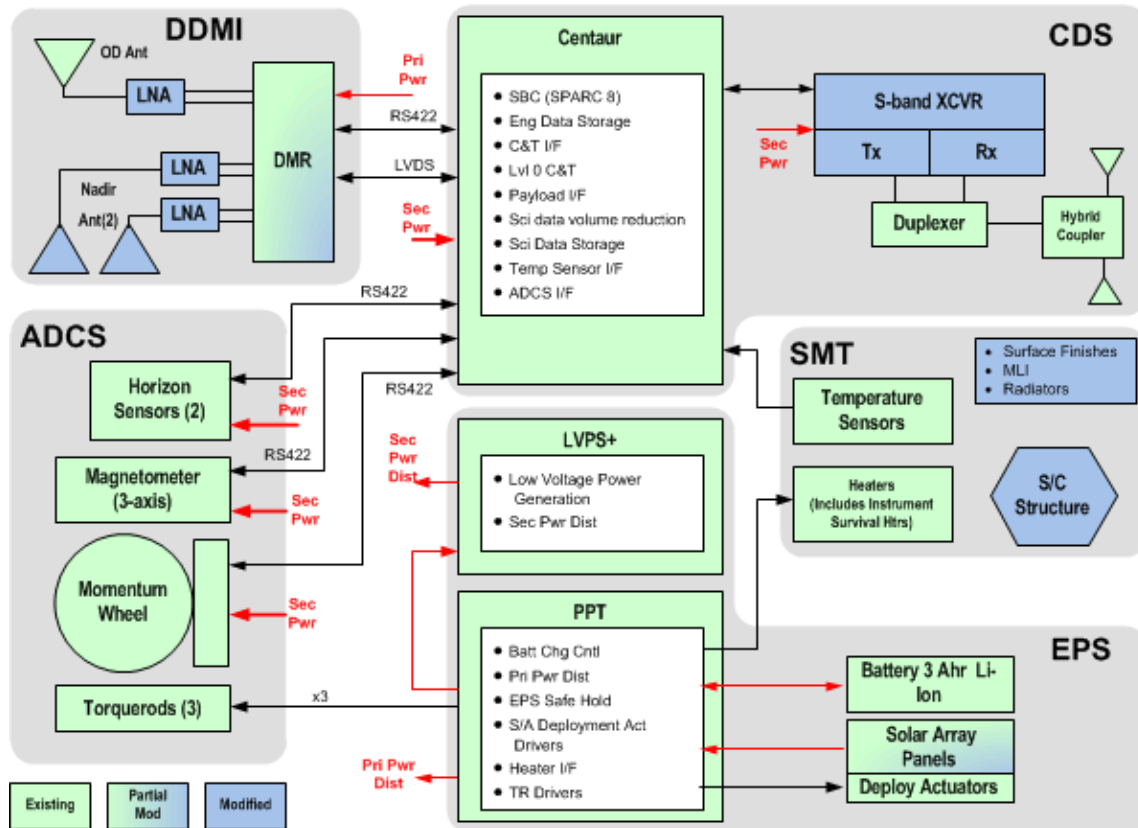


Figure 9 – CYGNSS single-string architecture

The thermal control design provides thermal stability while minimizing thermal gradients through an integrated design of multilayer insulation blankets (MLI), surface treatments, and localized radiators. The arrangement of internal equipment is used to aid thermal control and eliminate the need for supplemental heaters except for survival operations.

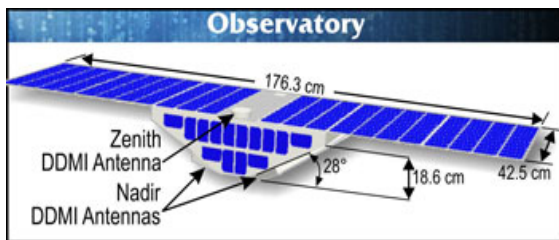


Figure 10 - CYGNSS observatory flight configuration

**Electrical Power**—The EPS is based on a  $28 \pm 4$  Vdc primary power bus with electrical power generated by a 8-panel rigid S/A. Launch accommodations provide 4 of the 8 panels to be “z-folded” for launch as described in Figure 11. Electrical power storage for eclipse operations is provided by 2 1.5 A-hr Li-ion batteries connected directly to the primary power bus. Battery

charge regulation for the CYGNSS EPS is a peak power tracking (PPT) type regulator. The TRL 6 PPT, developed using SwRI internal funds, matches S/A conductance to the observatory load through pulse-width modulation using an optimization control circuit that integrates S/A W-sec over a preset period of time.

**Command and Data**—The CYGNSS spacecraft avionics core is SwRI’s Centaur board. The Centaur consists of SwRI’s space-qualified heritage Atmel SPARC12 processor integrated with heritage CCSDS compliant C&T interface, instrument data interface, and ADCS interface designs. The simple operational nature of the GNSS instrument and science profile allows the command data subsystem to operate autonomously during all normal science and communication operations. Command services include COP-0 uplink command processing with BCH error detect and correction. The Centaur also provides FSW-independent execution of a Level-0 command set used for ground-based fault management. All other commands are passed to the FSW Command Manager for execution or to the Stored Command Sequence Manager as onboard Absolute and Relative Time Sequences.



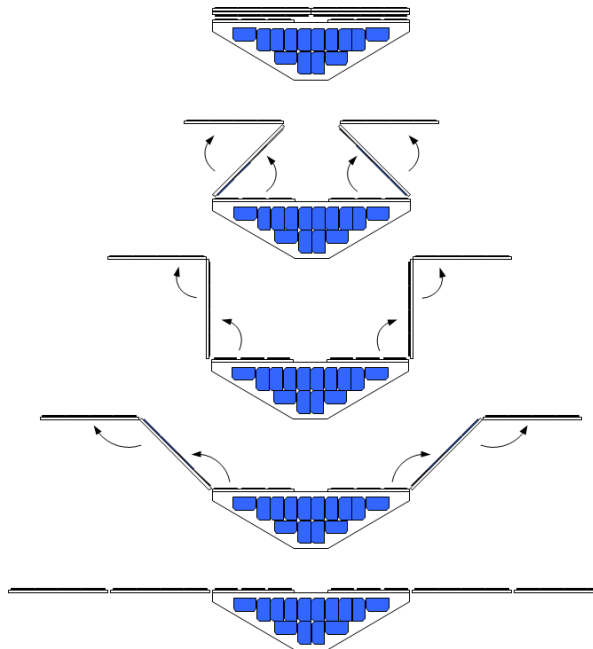


**Figure 11 – CYGNSS “z-fold” solar array provides exposed array while stowed and a balanced deployment to full power**

The FSW Telemetry Manager provides collection and high-level formatting of housekeeping data. These data are either downlinked in real-time or passed to the FSW Storage Manager to be stored for later downlink. A SwRI heritage H/W formatter forms CCSDS source packets into transfer frames and supports four separate Virtual Channel buffers to enable optimized data routing and processing within the CYGNSS Ground Data System. The heritage 4 GB Flash memory data store allows for >10 days of continuous science operations without downlink, providing significant margin for contingency operations.

S-band communication links are provided to uplink command sets and downlink science and H/K data. These links use two fixed omni-directional micro-strip patch antennas, one on the nadir baseplate and one on the zenith panel, to provide near  $4\pi$  sr communications without interrupting science operations.

The S-band transceiver uses SwRI’s low-cost, radiation-tolerant, single card communication solution. The core of the transceiver is a Software Defined Radio architecture configured to provide S-band (2 GHz) communications. The transceiver provides O-QPSK encoded transmit data at 1.25 Mbps with a FSK uplink receiver supporting data rates to 64 kbps.

*Attitude Determination and Control*—The CYGNSS ADCS is a standard nadir-pointing, 3-axis, pitch momentum- bias design using pitch/roll horizon sensors

and a 3-axis magnetometer for attitude determination with a pitch momentum wheel and 3-axis torque rods to provide attitude control (torque rods also provide momentum wheel desaturation).

*Automated Event Recognition (AER)* —On-board AER allows the CYGNSS Observatory to autonomously perform science operations while ensuring all subsystems operate within their safety limits. If subsystem data exceeds the predefined safety constraints, AER performs the designed response. The Safe mode (Figure 3) is configured for the DDMI to be powered off, providing 65% power margins to address anomalous conditions. Autonomous and on-board fault management responses are implemented using simple telemetry monitoring logic and stored command sequence capabilities. The heritage Centaur hardware design includes Watchdog provisions to monitor processor and FSW operations in addition to Level 0 command and telemetry capabilities that allow operators to monitor Observatory low level status and issue primary commands to reset the processor and shed power loads.

## SUMMARY

The CYGNSS mission implementation provides strong resiliency to unforeseen issues: reduced NRE using many “build-to-print” components, a simple Observatory operational concept allows mission operations to focus on monitoring the constellation; and system level redundancy that provides inherent fault tolerance and graceful system degradation/fault tolerance with only 7 of 8 Observatories required for baseline science. Our design provides strong contingencies and margins for all resources to allow flexibility to solve issues without compromising science goals.

The CYGNSS mission introduces a new paradigm in low-cost Earth science missions that employs a constellation of science-based  $\mu$ sats to fill a gap in capabilities of existing large systems at a fraction of the cost. CYGNSS will provide unprecedented coverage of winds within a TC throughout its life cycle thus providing critical data necessary for advancing the forecast of TC intensification.

## References

1. N. S. Foundation, "Hurricane Warning: The Critical Need for a National Hurricane Research Initiative, NSB-06-115," 2007.
2. National Oceanic and Atmospheric Administration, "Hurricane Forecast Improvement Project," 2008.

3. Borenstein, S., and Amario, C., "Irene forecasts on track; not up to speed on wind," Associated Press, 2011.
4. Katzberg, S. J., R.A. Walker, J. H. Roles, T. Lynch, and P. G. Black, "First GPS signals reflected from the interior of a tropical storm: Preliminary results from hurricane Michael," *Geophys. Res. Lett.*, 28, pp. 1981-1984, 2001.
5. Katzberg, S.J., Torres, O. and G. Ganoë. "Calibration of Reflected GPS for Tropical Storm Wind Speed Retrievals," *Geophys. Res. Lett.*, 33, L18602, doi:10.1029/2006GL026825, 2006.
6. Schlax, M. , Chelton, D. B., and Freilich, M. H., "Sampling Errors in Wind Fields Constructed from Single and Tandem Scatterometer Datasets," *Journal of Atmospheric and Oceanic Technology*, pp. 18, 1014–1036, 2001.
7. Rose, R., Dickinson, J., and Ridley, A., "CubeSats to NanoSats; Bridging the Gap between Educational Tools and Science Workhorses," in *IEEE Aerospace Conference, Big Sky, Montana*, 2012.
8. Zavorotny, V. U., and A. G. Voronovich, "Scattering of GPS signals from the ocean with wind remote sensing application," *IEEE Trans. Geosci. Remote Sensing*, 38, 951-964, 2000.
9. Gleason, S., Hodgart, S., Sun, Y., Gommenginger, C., Mackin, S., Adjrad M., and Unwin, M., "Detection and Processing of Bi-Statically Reflected GPS Signals From Low Earth Orbit for the Purpose of Ocean Remote Sensing," *IEEE Trans. Geoscience and Remote Sensing*, 43(5), 2005.
10. Gleason, S., "Remote Sensing of Ocean, Ice and Land Surfaces Using Bi-statically Scattered GNSS Signals From Low Earth Orbit," Ph.D. Thesis, University of Surrey (U.K.), January 2007.
11. Finley, T., Rose, D., Wells, W., Redfern, J., Nave, K., Rose, R., and Ruf, C., "Techniques for LEO Constellation Deployment and Phasing Utilizing Differential Aerodynamic Drag," *AIAA Astrodynamics Conference*, 2013.

